ELSEVIER

International Journal of Mass Spectrometry 194 (2000) 225–234

International Journal of Mass Spectrometry

Axial ion motion within the quadrupole ion trap elucidated by dc pulse tomography

Carsten Weil[a,1], J. Mitchell Wells[a], H. Wollnik[b], R. Graham Cooks[a,*]

[a]*Department of Chemistry, Purdue University, West Lafayette, IN 47907, USA*
[b]*II. Physikalisches Institut, Justus Liebig Universität, 35392 Gießen, Germany*

Received 28 April 1999; accepted 30 June 1999

Abstract

A new experimental technique is described for probing the motion of ions in a quadrupole ion trap via the application of short dc pulses to one endcap electrode. The method, which arose from simulations conducted using a multi-ion simulation program, ITSIM, reveals details of the motion of trapped ions and allows experimental measurement of the ion secular frequency. It is shown that a short dc pulse having the appropriate phase relationship with respect to the phase of oscillation of a population of trapped ions may be used to activate and eject chosen species from the trap while leaving other ions, even isobaric ions, relatively unperturbed. This provides a possible basis for high resolution collisional activation and high resolution mass analysis in the Paul trap. (Int J Mass Spectrom 194 (2000) 225–234) © 2000 Elsevier Science B.V.

Keywords: Quadrupole ion trap; Ion trap; Ion motion; Simulation; Secular frequency

1. Introduction

The quadrupole ion trap is a powerful mass spectrometer that has been significantly improved since its first commercial appearance as a gas chromatography detector in 1984 [1]. High resolution is available using slow scan rates [2–4], a mass/charge range of more than 70 000 Thomson (Th, unit of mass/charge, see [5]) has been demonstrated [6], and MS^n capabilities [7–9] are available. Further improvements in the performance characteristics of the ion trap, especially improvements in mass measurement accuracy, require a better understanding of the complexities of ion motion in the nonideal electric fields of real devices. Two complementary approaches have been used to study ion motion. One is to employ experiment, especially laser tomography experiments [10–12]. The second is to elucidate ion motion through computer modeling and simulation [13–18]. The work reported here utilizes both simulations and ion tomography, and introduces a new method for performing tomography experiments.

The earliest experiments that examined ion motion in quadrupole ion traps may have been those of Wuerker [19], who photographed macroscopic charged particles of aluminum and iron to follow their trajectories. In 1979 Knight and Prior [20] used

---

* Corresponding author.

[1] On leave from II. Physikalisches Institut, Justus Liebig Universität, 35392 Gießen, Germany.

Dedicated to Professor Jim Morrison, on the occasion of his 75th birthday and in admiration of his pursuit of excellence by combining instrumentation and chemistry.

PII S1387-3806(99)00151-7

laser-induced fluorescence to detect atomic ions and to determine the size of the trapped ion cloud. Laser photodissociation of trapped ions has formed the basis for a number of laser tomography studies [10–12,21] to determine the distribution of ions in the trap and to measure ion secular frequency. Efficient mass-selective laser photodissociation without isolation of the ions of interest has also been achieved [22]. The main disadvantage of these techniques is that they require that the electrodes of the ion trap be modified to allow optical access by the probe laser to the interior of the trap; this modification perturbs ion motion. For example, the large slots machined into the endcap electrodes to permit rastering of the probe laser beam in one experiment caused the chemical mass shift [23] for certain compounds to increase, a result that is attributable to the nonideal electric fields introduced by the slots [12]. A method of probing ion motion that does not require modification of the electrode structure, and the attendant disruption of the ion motion, is obviously desirable.

In this work, short (<1 μs) dc pulses were used to activate an ensemble of trapped ions to cause their partial or total ejection. Pulses of this type have been used previously to effect surface-induced dissociation (SID) in the quadrupole ion trap [24,25], and to activate ion populations in a broadband fashion for nondestructive detection [26]. Also, Dawson and Lambert [27], and more recently Lubman and coworkers [28], used a dc pulse to eject ions from a trap. Dawson and Lambert studied the effect of the rf phase of the pulse on the output signal, and supported their findings with ion trajectory calculations. The dc tomography experiments described here have the different aim of elucidating the motion of trapped ions and contributing to the development of higher resolution capabilities. They have the advantage over previous laser tomography experiments of yielding information about ion motion in a trap of *unmodified* geometry.

Dawson and Whetten [29] and March and coworkers [13,14] were the first to compute single ion trajectories in the quadrupole ion trap. Julian et al. [30] first computed trajectories for large ensembles of ions and generated mass spectra by simulating the mass-selective instability scan [1] using a parallel computer. The development of the quadrupole ion trap simulation program ITSIM [16] in our laboratory has facilitated multi-ion simulations using single-processor personal computers by dividing the simulation process into three subunits—ion generation, ion motion calculation, and data extraction, and following the motion of individual ions through a sequence of time intervals. The current Windows version of the ITSIM program [17,31] is capable of simulating the effects of auxiliary ac and dc fields, in addition to the main rf trapping field, on the motion of large ensembles of ions. Ion trajectories are computed using either the Euler or Runge-Kutta integration methods at intervals that are short compared to the rf oscillation period. In addition, ion/neutral collisions [16] and ion/ion interactions are available in the program and can be utilized in particular simulations. The effects of nonideal fields on ion motion can be simulated either by expressing the field analytically, as a multipole expansion [32], or by a numerical representation of the electric potential [23]. ITSIM offers many kinds of displays to illustrate the simulated data. The most common display of the trajectory information is to divide ion excursions in the x-, y-, and z-directions and plot them individually versus time. The total kinetic energy of each ion, as well as the phase angle and potentials of the rf, may be plotted also. Many helpful tools such as phase space plots and Poincaré plots are available. Production and display of four-dimensional data sets (spatial distributions in x-, y-, and z-directions and time) are available, and all these capabilities greatly assist in understanding the motion of ions at any time during a simulation.

2. Experimental

The instrument used to perform these experiments was a prototype Finnigan ion trap mass spectrometer (ITMS), which is described elsewhere [7]. The main change in the instrumentation was the use of an external rf frequency oscillator to generate the 1.1 MHz rf reference signal. The single high frequency oscillator of the ITMS was replaced by two Hewlett-

Packard frequency synthesizers (HP 33120A, Hewlett Packard, Palo Alto, CA). One generator produced the fixed 1.1 MHz drive frequency while the second generated the auxiliary ac frequency used for ion excitation. The 1.1 MHz external rf frequency from the first frequency synthesizer was connected to the ITMS motherboard via a CMOS interface. This rf oscillator was coupled to the ac reference input of the second frequency synthesizer, so that the two signals were generated from the same clock. This arrangement allowed the rf and ac signals to have the desired fixed-phase relationship. A home-built high voltage dc pulser [33] based on a DEI HV1000 fast pulse switch (Directed Energy, Inc., Fort Collins, CO) was used to probe ion motion. This pulse was phase-locked to the rf trapping voltage using a home-built piggyback circuit [33] so that the dc pulse could be applied precisely at any desired rf phase angle. The ability to control the phase relationship between rf, ac, and dc is an important criterion for the success of these experiments, as described below. The dc pulser was connected to one endcap of the ion trap via a 50 Ω load.

Krypton or benzene-d_6 was leaked into the ITMS manifold through a variable leak valve (Granville-Phillips, Boulder, CO) to a pressure of between 2 and 6×10^{-6} Torr (uncorrected) as measured on a Bayert-Alpert type ionization gauge. Helium buffer gas was used in some experiments, as indicated below, at a pressure of 2×10^{-4} Torr (uncorrected). The scan function began with a period of electron ionization, typically of 0.5 ms. The ion of interest was then isolated using rf/dc isolation at the apex ($a_z = 0.150$, $q_z = 0.7815$) of the Mathieu stability diagram and allowed to cool for 4 ms at the desired q_z-value, which was chosen so that the rf frequency was an exact multiple of the ion secular frequency (see discussion below). The frequency synthesizer used for ac excitation was triggered by a signal derived from the ITMS and controlled by the ITMS data system. For ac ion excitation experiments, the ac frequency was applied to one endcap electrode for 240 μs. The dc pulse was then applied to the other endcap to remove some or all of the excited ion population, as described in the next section. The start time of the dc pulse application was precisely controlled using a digital delay generator (Model DG535, Stanford Research Systems, Inc., Sunnyvale, CA). The scan function ended with an rf mass analysis scan [1], and the ions were detected with a conversion dynode/electron multiplier assembly. The signal from the ITMS preamplifier was measured using a digital oscilloscope (TDS 540, Tektronix, Beaverton, OR).

3. Results and discussion

Fig. 1 shows the results of a simulation of the motion of 20 ions of 100 Th in the trap at $q_z = 0.639315$ ($\beta_z = 0.500000$, secular frequency $f_z = 275.000$ kHz). To simulate the results of ac excitation without the need to repeat this step in every simulation, the ion spatial distribution in the z-dimension was determined after simulating the activation of a cooled ion population residing in the center of the ion trap with a dipolar ac potential of 275 kHz and 2 V for 100 μs. The spatial distribution of this excited ion population was recorded at the turning point of the ion cloud in the z-dimension, and this distribution was then used as the input spatial distribution for all subsequent simulations. Note that in all simulations, the ions were started with no displacement in the radial dimension and with zero initial velocity in both dimensions. In Fig. 1(a), a dipolar dc pulse of 227 ns and 400 V is applied 9.67 μs after the start of the simulation. The phase relationship between the dc pulse, the ions' oscillation in the z-direction, and the rf trapping voltage is such that the pulse rapidly increases the excursion in the z-dimension, causing ion removal from the trap ~0.7 μs after the end of the pulse. In Fig. 1(b), the dc pulse has the same width and amplitude, but is applied 10.13 μs after the start of the simulation; the effects of the pulse on the ion motion have changed dramatically. Now the pulse actually removes some of the kinetic energy given to the ions by the ac excitation, decreasing their excursion in the z-dimension. This observation suggests that it may be possible to use short dc pulses to effect electrical cooling of ions in the ion trap. However, this method of electrically cooling the ions requires that

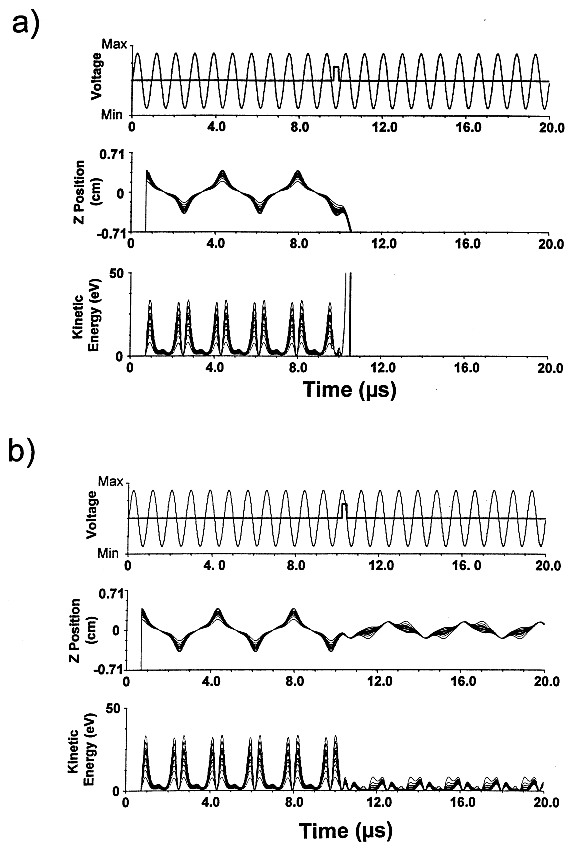

Fig. 1. Simulation of the motion of 20 ions having a *m/z* ratio of 100 Th at a q_z-value of 0.639 315, generated with a distribution in the *z*-dimension consistent with excitation via a dipolar ac potential (see text). The dc pulse is 227 ns long and 400 V in amplitude. (a) dc pulse applied 9.67 μs after the start of the simulation, resulting in excitation and removal of all ions. (b) dc pulse applied 10.13 μs after the start of the simulation, resulting in *z*-axis cooling of the ion cloud with no ion loss.

the ion cloud be moving coherently, i.e. the ions must be heated, using the ac in this experiment, before they can then be cooled; the net result is that the ions still have more kinetic energy after the cooling than they had before they were excited into coherence. Further investigation of this and other electrical cooling methods is ongoing. The large peaks in the kinetic energy plots in Fig. 1 are due to the rf micromotion, which at this high q_z-value contributes more to the ion velocity than does the secular motion.

The sensitivity of ion removal to the phase of the dc pulse compared to that of ion oscillation and that of rf voltage is the basis for the dc tomography experiment. Fig. 1 shows the two extreme situations, complete removal and complete retention of the ion cloud. A range of intermediate conditions also exists for other dc pulse amplitudes and phases where only a portion of the ion cloud is removed. If the dc pulse is sufficiently short and the application time is changed in increments that are also sufficiently small, relative to the period of the ion secular motion and the rf trapping potential, and if there is a fixed-phase relationship between the ion motion, the rf trapping voltage, and the dc pulse, a plot of ion number left in the trap versus dc pulse application time yields a plot of the secular motion of the ion cloud in the *z*-dimension. The phase relationship between the ion motion and the rf trapping voltage is fixed in the simulation by always creating the ions with the same distribution and at the same point in the rf cycle at a q_z-value for which the secular frequency is an exact fraction of the rf frequency.

Fig. 2 illustrates the results of the implementation of such a dc tomography experiment. In the experiment, the required phase relationship is achieved by fixing the phase relationship between the rf trapping voltage and the ac excitation potential, as described in the experimental section. To maintain a fixed-phase relationship between the ac and the rf it is required that the ac frequency be an exact fraction of the rf frequency, hence the choices of $q_z = 0.345$ and 0.14, where the secular frequencies are 137.5 and 55 kHz, respectively, in the experiments described below. The helium buffer gas pressure for these experiments was 2×10^{-4} Torr (uncorrected). The experimental data in Fig. 2(a) were recorded for the 84 Th isotope of krypton, present in the trap at $q_z = 0.345$. The ions were excited using a dipolar ac signal of 137.5 kHz with an amplitude of 0.5 V. The dc pulse was first applied 300 μs after the end of the period of ac excitation, and was 350 ns long and 250 V in amplitude. The dc pulse width and amplitude were held constant during the course of the experiment, and the start time was increased in increments of 100 ns. The amplitude of the 84 Th signal remaining in the trap upon mass analysis was recorded and is plotted as a function of dc pulse start time in Fig. 2(a). Three

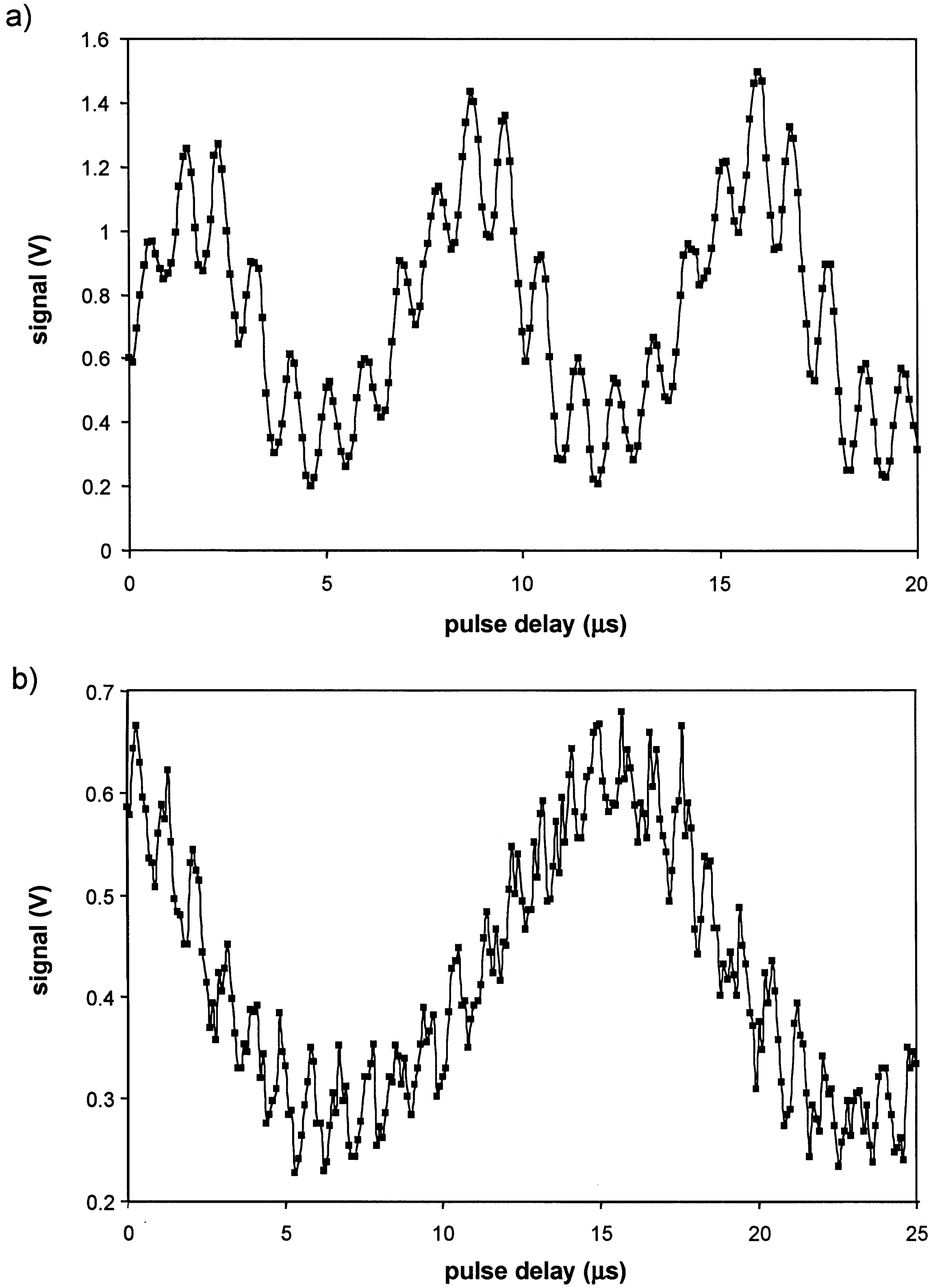

Fig. 2. Secular oscillations of krypton (84 Th) recorded using the dc tomography method, after excitation of the ions with an ac voltage of appropriate frequency, at (a) $q_z = 0.345$ and (b) $q_z = 0.14$. In the first experiment, the start time of the dc pulse ($t = 0$) was 300 μs after the end of the ac excitation; the times on the x-axis are referenced to this dc pulse.

cycles of the ion secular motion are evident in the figure. The secular frequency can be measured from these data. There are an insufficient number of data points to allow a Fourier transformation of the data to yield an accurate measure of the secular frequency. However, Fourier transform techniques were used to remove the higher frequency components, improving the accuracy of the period measurement. The data were Fourier transformed, the amplitude and the phase of all frequency components except those that bracketed the estimated frequency of ion motion were set to zero, and the inverse Fourier transform was then taken. The data thus filtered were plotted and the period of the oscillations was determined by measuring the distance between adjacent peaks and adjacent valleys. The secular frequency determined in this way was 137 kHz ± 0.7 kHz, which is in good agreement with the theoretical value of 137.5 kHz calculated for an ion trap with a ring electrode radius r_0 of 1.0 cm and a center-to-endcap spacing z_0 of 0.783 cm, i.e. the standard commercial geometry ion trap used in the Finnigan ITMS, ITD, ITS40, and Magnum systems [34].

Fig. 2(b) illustrates the results of the same experiment at a q_z value of 0.14. In this experiment the dc pulse was lowered to an amplitude of 50 V because of the shallower quasipotential well at this lower q_z-value. One-and-a-half secular cycles were recorded, and the secular frequency was measured to be 56 ± 0.7 kHz, which is higher than the theoretical value of 55 kHz, again calculated for a commercial geometry ion trap.

It was shown previously [35–37] that the optimum excitation frequency for effecting collision-induced dissociation (CID) in the ion trap can differ from the theoretical frequency by several hundred hertz. The nonideal electric fields that exist in real traps due to electrode apertures and truncation have been shown to cause frequency shifts [38–40] that may explain the small discrepancies between the experimental and theoretical frequencies. In some particular cases, e.g. for the molecular ion of nitrobenzene, it has been shown that nonideal fields combined with collisions with bath gas can cause even larger shifts in peak position [23]. Ion-ion coulombic interactions, normally referred to as space charge effects, are known to degrade the mass accuracy of ion trap mass spectrometers by delaying ion ejection, even when ion numbers are kept very low [41]. This effect can be attributed to the net positive dc potential caused by the ion cloud [42], which in effect causes a shift of the stability diagram [43]. Such a shift lowers the secular frequency of the ions. Space charge effects are easily studied by changing the ionization time and interrogating ion motion with dc tomography. Further testing of the effects of nonideal fields on peak positions will be conducted using the dc tomography technique to study the effect of the ion trap z_0-dimension on ion motion in a custom built, adjustable-z_0 ion trap, which has been described previously [44].

Also evident in the data shown in Fig. 2 is a lower amplitude signal with a frequency of 1.1 MHz that overlays the secular motion at both q_z values. This signal is due to the phase relationship between the dc pulse and the rf trapping voltage, and it also influences ion removal. This effect is seen more clearly in Fig. 3, where all parameters are the same as for Fig. 2(a) except that the delay between ion excitation and interrogation by the dc pulse has been increased from 300 μs to 3 ms. In the presence of 2×10^{-4} Torr (uncorrected) of helium buffer gas, the ions have cooled to the center of the trap after 3 ms, so that their secular oscillations are too small to observe. Only the 1.1 MHz oscillation, which is due to the phase of the dc pulse with respect to the rf voltage, is visible. If the dc/rf phase is such that the sign of the rf voltage opposes ion removal by the dipolar dc pulse, for example, when the endcaps are positive relative to the ring electrode in the case of positive ions, then fewer ions are removed than in cases where the dc/rf phase favors ion removal. This sensitivity of ion removal to the dc/rf phase shows up in the data as the 1.1 MHz oscillation evident in Figs. 2 and 3. Comparison of Figs. 2 and 3 also illustrates that the dc pulse tomography method can be used to study ion cooling. It might be possible to differentiate between ions with different cooling times and hence different collision cross sections, i.e. to perform an ion mobility experiment [45] in the ion trap. This was achieved recently as reported in another publication [46].

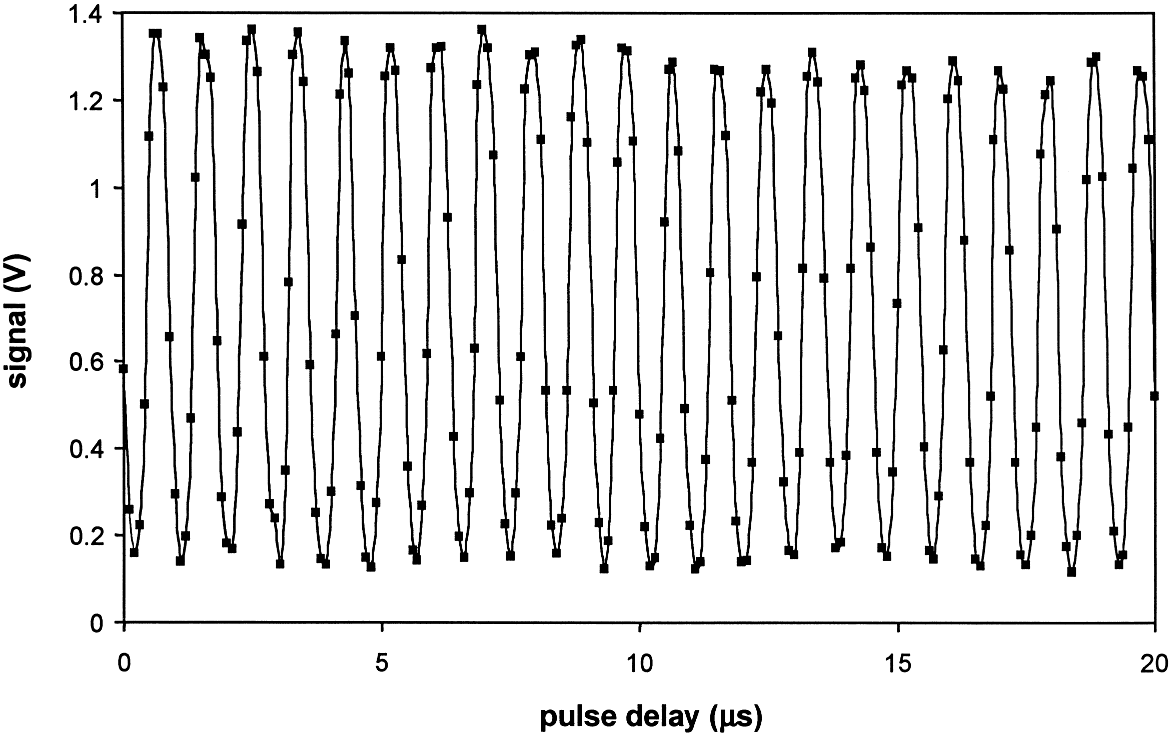

Fig. 3. dc tomography of krypton (84 Th) recorded at $q_z = 0.345$. The application time of the dc pulse ($t = 0$) was 3 ms after the end of the ac excitation period; the times on the x-axis are those of the dc pulses used in the set of experiments referenced to this earliest dc pulse. Note that no secular oscillations are observable after the 3 ms cooling time (see text).

The dc tomography technique can also be extended to high resolution isolation of ions in the ion trap. Two ion populations that are close in mass/charge ratio will oscillate with very similar frequencies. After the ion populations have begun to oscillate at their characteristic frequencies, they will be 180° out of phase after a period of time determined by their difference in frequency as shown in Eq. (1):

$$t_{180} = \frac{1}{2}\left(\frac{1}{f_z(a) - f_z(b)}\right), \tag{1}$$

where $f_z(a)$ is the secular frequency of the lower mass ion and $f_z(b)$ is the secular frequency of the higher mass ion. Fig. 4 illustrates how a fast dc pulse can be used in conjunction with this phase shift to effect high resolution isolation. In this simulation, ion populations with *m/z* ratios 100.000 and 100.001 Th were created and trapped under identical conditions, viz. at q_z values of 0.639 315 and 0.639 309, respectively. The ions have a frequency difference of 4 Hz, so they acquire a 180° phase difference 125 ms after excitation. The simulation shown here begins with the ions at this phase difference and with the distribution in the z-dimension determined as described above. A 227 ns, 400 V dc pulse is applied 10.34 μs after the start of the simulation. The pulse phase with respect to the ion motion and the rf trapping voltage is such that the ions of *m/z* 100.001 are completely removed from the ion trap while the *m/z* 100.000 ions are cooled slightly and completely retained.

The simulation in Fig. 4 represents a resolution in terms of ion isolation in excess of 100 000. However, it must be noted that there are a number of factors that would make this value difficult to achieve experimentally. Coupling of ion motion for ions of similar mass is well known in magnetic traps [47–50] and has been

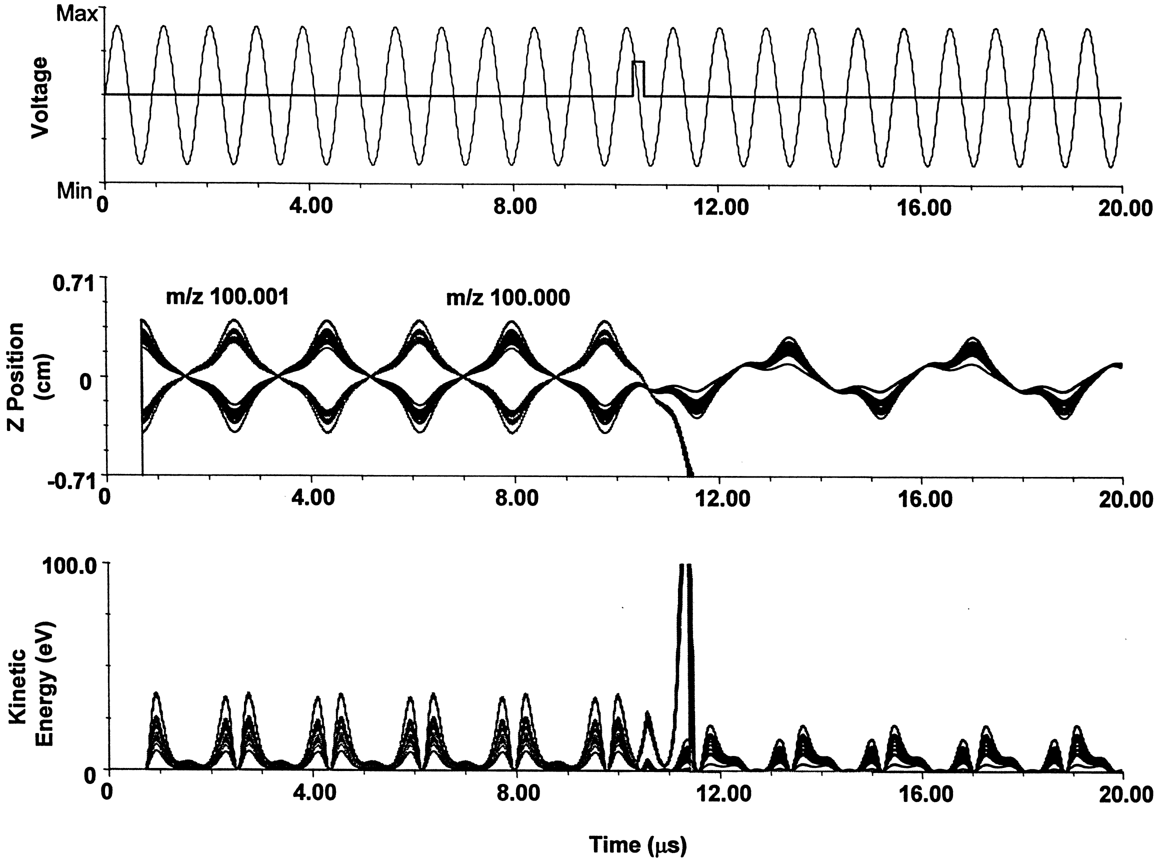

Fig. 4. Simulation of the motion of 20 ions of *m/z* 100.000 and 20 ions of *m/z* 100.001, generated at $q_z = 0.639$ with a 180° phase difference, illustrating the principle of high resolution isolation of *m/z* 100.000 using dc tomography.

observed in quadrupole ion traps as well [36,51], and has been shown to increase in strength as the difference in ion mass decreases [51]. Such coupling could prevent the ion populations from oscillating out of phase. Also, collisions with residual background gas would dephase ion motion during the 125 ms delay, possibly to such an extent that differentiation of the species would be impossible.

Fig. 5 shows the results of an experiment in which krypton and benzene-d_6, which both produce ions with a nominal *m/z* of 84 Th, were consecutively admitted into the trap and studied via dc tomography. No helium buffer gas was used during this experiment. The exact mass of the mass 84 isotope of krypton is 83.91 Da, while the molecular ion of benzene-d_6 has a mass of 84.16 Da. When the rf amplitude is set so that the low mass cutoff is at 31.9 Th, to place nominal 84 Th at $q_z = 0.345$, the q_z of the krypton ion is 0.345 319 and its frequency is 137.598 kHz, as calculated for a commercial geometry ion trap. The benzene molecular ion has a q_z of 0.344 168 and its frequency is 137.168 kHz, again as calculated for a commercial geometry ion trap. The mass difference causes these two isobaric *m/z* 84 ions to have a frequency difference of 430 Hz, which should cause the ion clouds to oscillate 180° out of phase 1.16 ms after excitation. The dc tomography results in Fig. 5 show very good agreement with this hypothesis. The peak in the benzene-d_6 signal at time 1.19 ms corresponds almost exactly to the valley in the krypton signal seen at the same time, indicating that these two species are oscillating out of phase after

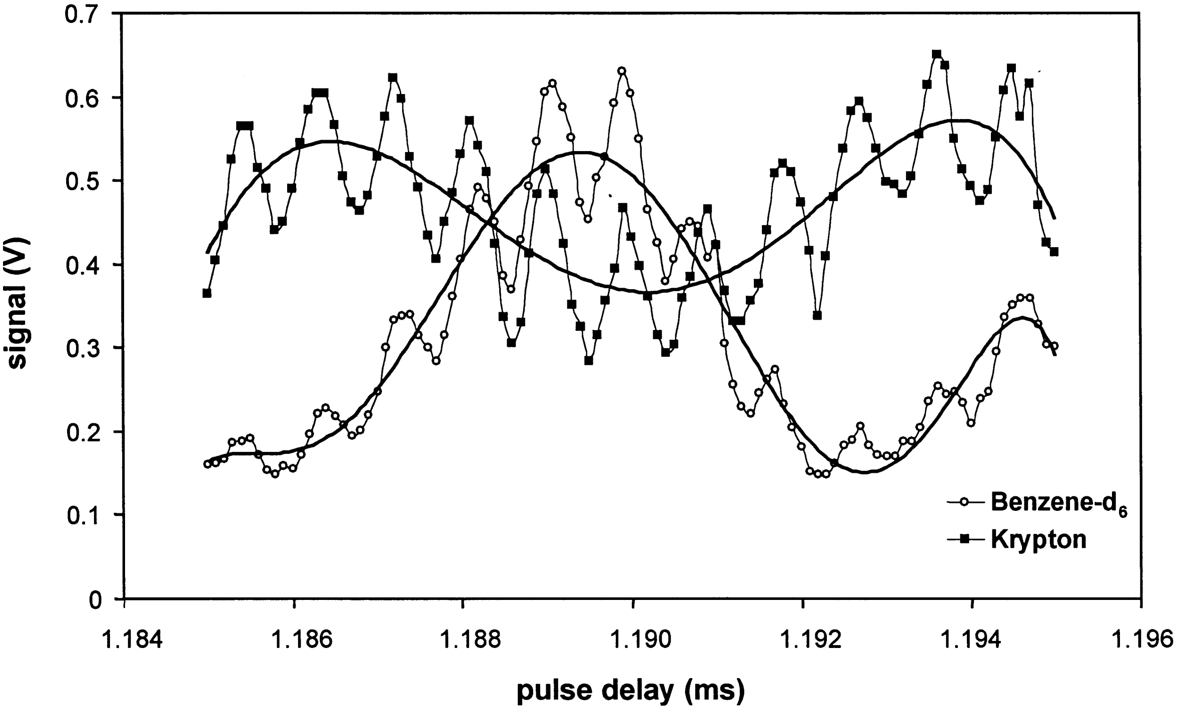

Fig. 5. dc tomography of krypton (84 Th) and the molecular ion of benzene-d_6 (84 Th) recorded separately and plotted on the same time axis. The application time of the earliest dc pulse was 1.185 ms after the end of the ac excitation; note that in this figure, the pulse application times are referenced to the end of the ac excitation, and not to the earliest dc pulse, to emphasize that ~1.2 ms is needed after excitation for the ions to oscillate 180° out of phase. The heavy lines are polynomial fits intended as guides in examining the data.

1.19 ms. This corresponds to an actual frequency difference of 420 Hz. If the two species had been present in the trap at the same time, the dc pulse applied at 1.19 ms would have removed more of the krypton ions than the benzene ions, i.e. the benzene ions would have been isolated from the isobaric krypton ions, provided that the ion merging problem discussed above could be avoided. These trial experiments have prepared the way for higher resolution measurements in which krypton and benzene-d_6 are simultaneously introduced.

4. Conclusions

The dc tomography technique can be used to probe ion motion in the quadrupole ion trap without any modification to the physical structure of the trap. Preparatory experiments and theory on the use of fast dc pulses to achieve high resolution isolation and activation of ions in the trap have been presented. These pulsed methods have also been shown to cause z-axis cooling when the pulse phase is appropriate. We note also that it is possible to excite ions with a fast dc pulse [24,25] instead of the ac excitation used in the simulations and experiments reported above. Hence, it is possible to perform the dc tomography method with two dc pulses, rather than in the ac/dc fashion described here. Simulations suggest that the results of dc tomography experiments depend on the spatial distribution of the ion cloud, and so future work will involve developing dc tomography as a means of studying this spatial distribution. The ability to achieve high resolution isolation and mass analysis with the dc tomography technique will also be pursued, as will the electrical cooling phenomenon encountered in phase-coherent ion populations.

Acknowledgements

The authors thank Dr. Lynn Gill for her contributions to this work and acknowledge the financial support of the United States Department of Energy (DE-FG02-94ER14470), the Office of Naval Research (N00014-94-K-2002), and Finnigan Corporation through the Purdue University Industrial Associates program.

References

[1] G.C. Stafford, P.E. Kelley, J.E.P. Syka, W.E. Reynolds, J.F.J. Todd, Int. J. Mass Spectrom. Ion Processes 60 (1984) 85.

[2] F.A. Londry, G.J. Wells, R.E. March, Rapid Comm. Mass Spectrom. 7 (1993) 43.

[3] J.D. Williams, K.A. Cox, R.G. Cooks, R.E. Kaiser, J.C. Schwartz, J. Am. Soc. Mass Spectrom. 5 (1991) 327.

[4] I.J. Amster, Rapid Commun. Mass Spectrom. 7 (1993) 210.

[5] R.G. Cooks, A.L. Rockwood, Rapid Commun. Mass Spectrom. 5 (1991) 93.

[6] R.E. Kaiser, R.G. Cooks, G.C. Stafford, J.E.P. Syka, P.H. Hemberger, Int. J. Mass Spectrom. Ion Processes 106 (1991) 79.

[7] J.N. Louris, R.G. Cooks, J.E.P. Syka, P.E. Kelley, G.C. Stafford, J.F.J. Todd, Anal. Chem. 59 (1987) 1677.

[8] J.N. Louris, J.S. Brodbelt-Lustig, R.G. Cooks, G.L. Glish, G.J. VanBerkel, S.A. McLuckey, Int. J. Mass Spectrom. Ion Processes 96 (1990) 117.

[9] S.A. McLuckey, G.L. Glish, G.J. VanBerkel, Int. J. Mass Spectrom. Ion Processes 106 (1991) 213.

[10] P.H. Hemberger, N.S. Nogar, J.D. Williams, R.G. Cooks, J.E.P. Syka, Chem. Phys. Lett. 191 (1992) 405.

[11] J.D. Williams, R.G. Cooks, J.E.P. Syka, P.H. Hemberger, N.S. Nogar, J. Am. Soc. Mass Spectrom. 4 (1993) 792.

[12] C.D. Cleven, R.G. Cooks, A.W. Garrett, N.S. Nogar, P.H. Hemberger, J. Phys. Chem. 100 (1996) 40.

[13] R.E. March, A.W. McMahon, F.A. Londry, R.L. Alfred, J.F.J. Todd, F. Vedel, Int. J. Mass Spectrom. Ion Processes 95 (1989) 119.

[14] R.E. March, A.W. McMahon, E.T. Allinson, F.A. Londry, R.L. Alfred, J.F.J. Todd, F. Vedel, Int. J. Mass Spectrom. Ion Processes 99 (1990) 109.

[15] R.E. March, F.A. Londry, R.L. Alfred, J.F.J. Todd, A.D. Penman, F. Vedel, M. Vedel, Int. J. Mass Spectrom. Ion Processes 110 (1991) 159.

[16] R.K. Julian, M. Nappi, C. Weil, R.G. Cooks, J. Am. Soc. Mass Spectrom. 6 (1995) 57.

[17] H.A. Bui, R.G. Cooks, J. Mass Spectrom. 33 (1998) 297.

[18] D. Gerlich, Physica Scripta, T59 (1995) 256.

[19] R.F. Wuerker, H. Shelton, R.V. Langmuir, J. Appl. Phys. 30 (1959) 342.

[20] R.D. Knight, M.H. Prior, J. Appl. Phys. 50 (1979) 3044.

[21] S.A. Lammert, C.D. Cleven, R.G. Cooks, J. Am. Soc. Mass Spectrom. 5 (1994) 29.

[22] C.D. Cleven, M. Nappi, R.G. Cooks, A.W. Garrett, N.S. Nogar, P.H. Hemberger, J. Phys. Chem. 100 (1996) 5205.

[23] J.M. Wells, W.R. Plass, G.E. Patterson, Z. Ouyang, E.R. Badman, R.G. Cooks, Anal. Chem. 71 (1999) 3405.

[24] S.A. Lammert, R.G. Cooks, Rapid Commun. Mass Spectrom. 6 (1992) 528.

[25] S.A. Lammert, Ph.D Thesis, Purdue University, 1992.

[26] M. Soni, V. Frankevich, M. Nappi, R.E. Santini, J.W. Amy, R.G. Cooks, Anal. Chem. 68 (1996) 3314.

[27] P.H. Dawson, C. Lambert, Int. J. Mass Spectrom. Ion Phys. 14 (1974) 339.

[28] S.M. Michael, B.M. Chien, D.M. Lubman, Anal. Chem. 65 (1993) 2614.

[29] P.H. Dawson, N.R. Whetten, J. Vac. Sci. Technol. 5 (1968) 11.

[30] R.K. Julian, H.P. Reiser, R.G. Cooks, Int. J. Mass Spectrom. Ion Processes 123 (1993) 85.

[31] H.-P. Reiser, R.K. Julian, R.G. Cooks, Int. J. Mass Spectrom. Ion Processes 121 (1992) 49.

[32] R.E. March, R.J. Hughes, Quadrupole Storage Mass Spectrometry, Wiley, New York, 1989.

[33] S.A. Lammert, R.G. Cooks, J. Am. Soc. Mass Spectrom. 2 (1991) 487.

[34] J.E.P. Syka, in: R.E. March, J.F.J. Todd (Eds.), Practical Aspects of Ion Trap Mass Spectrometry, CRC, Boca Raton, FL, 1995, Vol. 1, p. 169.

[35] J.D. Williams, K.A. Cox, R.G. Cooks, S.A. McLuckey, K.J. Hart, D.E. Goeringer, Anal. Chem. 66 (1994) 725.

[36] W. Mo, J.F.J. Todd, Rapid Commun. Mass Spectrom. 10 (1996) 424.

[37] M. Splendore, M. Lausevic, Z. Lausevic, R.E. March, Rapid Commun. Mass Spectrom. 11 (1997) 228.

[38] J. Franzen, Int. J. Mass Spectrom. Ion Processes 106 (1991) 63.

[39] Y. Wang, J. Franzen, K.P. Wanczek, Int. J. Mass Spectrom. Ion Processes 124 (1993) 125.

[40] J. Franzen, Int. J. Mass Spectrom. Ion Processes 130 (1994) 15.

[41] K.A. Cox, C.D. Cleven, R.G. Cooks, Int. J. Mass Spectrom. Ion Processes 144 (1995) 47.

[42] E. Fischer, Z. Phys. 156 (1959) 1.

[43] J.E. Fulford, D.N. Hoa, R.J. Hughes, R.E. March, R.F. Bonner, G.J. Wong, J. Vac. Sci. Technol. 17 (1980) 829.

[44] L.A. Gill, J.W. Amy, W.E. Vaughn, R.G. Cooks, Int. J. Mass Spectrom. 188 (1999) 87.

[45] D.E. Clemmer, M.F. Jarrold, J. Mass Spectrom. 32 (1997) 577.

[46] W.R. Plass, L.A. Gill, R.G. Cooks, manuscript in preparation.

[47] J. Huang, P.W. Tiedemann, D.P. Land, R.T. McIver, J.C. Hemminger, Int. J. Mass Spectrom. Ion Processes 134 (1994) 11.

[48] J.S. Anderson, D.A. Laude, Int. J. Mass Spectrom. Ion Processes 157/158 (1996) 163.

[49] Y. Naito, M. Inoue, Int. J. Mass Spectrom. Ion Processes 157/158 (1996) 85.

[50] J.T. Stults, Anal. Chem. 69 (1997) 1815.

[51] K. Jungmann, J. Hoffnagle, R.G. DeVoe, R.G. Brewer, Phys. Rev. A 36 (1987) 3451.